FOA Rapport
C 20295-E4
Mars 1979

SWEDISH EARTHQUAKES AND ACCELERATION PROBABILITIES

Ragnar Slunga

FOA RAPPORTKATEGORIER

Rapporter avsedda för spridning utanför FOA utges i följande kategorier:

FOA A-rapport. Innehåller huvudsakligen för totalförsvaret avsedd och tillrättalagd redovisning av ett, som regel avslutat, arbete. Förekommer som öppen (A-) och hemlig (AH-) rapport.

FOA B-rapport. Innehåller för vidare spridning avsedd redovisning av öppet, vetenskapligt eller tekniskt-vetenskapligt originalarbete av allmänt intresse. Utges i FOA skriftserie »FOA *Reports*» eller publiceras i FOA utomstående tidskrift, i vilket senare fall särtryck distribueras av FOA under benämningen »*FOA Reprints*».

FOA C-rapport. Innehåller för spridning inom eller utom FOA (i vissa fall enbart inom FOA) avsedd redovisning av arbete, t ex i form av delrapport, preliminärrapport eller metodikrapport. Förekommer som öppen (C-) och hemlig (CH-) rapport.

FOA-RAPPORTS STATUS

FOA-rapports status är att författaren (författarna) svarar för rapportens innehåll, t ex för att angivna resultat är riktiga, för gjorda slutsatser och rekommendationer etc.

FOA svarar – genom att rapporten godkänts för utgivning som FOA-rapport – för att det redovisade arbetet utförts i överensstämmelse med vetenskap och praxis på ifrågavarande område.

I förekommande fall tar FOA ställning till i rapporten gjorda bedömningar etc; detta anges i så fall i särskild ordning, t ex i missiv.

REGISTRERING

Fr o m 1974-07-01 registreras FOA-rapport enligt följande exempel:

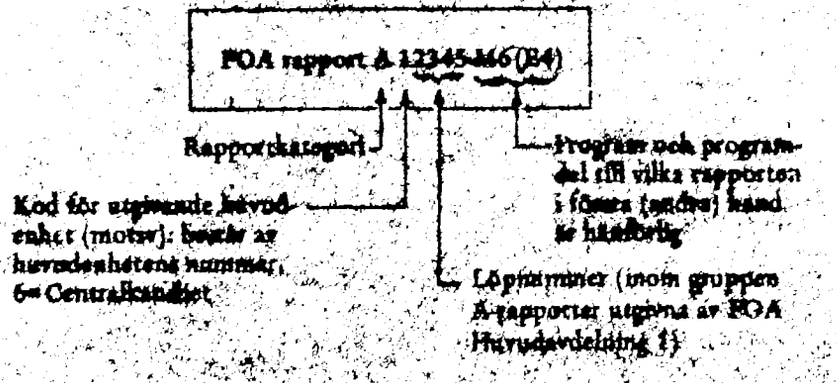

Försvarets Forskningsanstalt
Huvudavdelning 2
104 50 Stockholm

FOA rapport C 20295-E4
Mars 1979

SWEDISH EARTHQUAKES AND ACCELERATION PROBABILITIES

Ragnar Slunga

Antal sidor 48

Summary

A method to assign probabilities to ground accelerations for Swedish sites is described. As hardly any nearfield instrumental data is available we are left with the problem of interpreting macroseismic data in terms of acceleration. Although the correlation between intensity and ground acceleration is poor, the large amount of data collected from several regions gives regression lines with small estimated uncertainties. However, application of these lines to regions of no such data is necessarily very uncertain. This cannot be avoided until relevant instrumental data will be available.

When calculating the probabilities we want to define our earthquake model in physically simple concepts. Instead of working with intensity and radius of perceptability we transform these quantities to a seismic strength measure (magnitude measure) and focal depth. This transformation is based on wave propagation computations for a realistic crustal model. We then found that most Swedish earthquakes have a focal depth less than 25 km. The largest earthquake of the area, the 1904 eartquake 100 km south of Oslo, is an exception and probably had a focal depth exceeding 25 km.

The theoretical wave propagation computations also give the distance dependence of the elastic waves radiated by the eartquake sources. This knowledge is needed for calculating the probability to exceed a given acceleration.

Basic idea in the probability computation is the assumtion of uniform distribution of epicenters. This uniform distribution is estimated in a systematically conservative manner for each site. The reason for working with uniform distribution is lack of knowledge of the source processes involved. We also assume that magnitudes, focal depths and epicenters are uncorrelated.

For the nuclear power plant sites an annual probability of 10^{-5} has been proposed as interesting. This probability gives ground accelerations in the range 5-20 % for the sites. This acceleration is for a free bedrock site. For consistency all acceleration results in this study are given for bedrock sites.

When applicating our model to the 1904 earthquake and assuming the focal zone to be in the lower crust we get the epicentral acceleration of this earthquake to be 5-15 % g.

The results above are based on an analyses of macroseismic data as relevant instrumental data is lacking. However, the macroseismic acceleration model deduced in this study gives epicentral ground acceleration of small Swedish earthquakes in agreement with existent distant instrumental data.

Sammanfattning

En metod att bestämma sannolikheten för markaccelerationer beskrivs. Avsaknaden av instrumentella mätningar medför att makroseismiska observationer måste användas. Genom teoretiska vågutbredningsberäkningar framtages samband mellan skalvstyrka, fokaldjup, avstånd och maximalacceleration. Dessa relationer ger tillsammans med jordskalvsstatistik en modell för sannolikhetsberäkningar. Sannolikheten 10^{-5} per år ger därvid markaccelerationer på 5-20 % g för de kärnkraftsaktuella platserna. Om vågutbredningsmodellen tillämpas på 1904 års skalv fås en epicenteracceleration på 5-15 % g. Den modell vi här tagit fram baserad på makroseismiska observationer stämmer väl med de befintliga instrumentella mätningarna på större avstånd.

Uppdragsnr: E4 85

Sändlista: FÖD, Fst, ÖEF, FortF, SkyddS, Cfs (3 ex), Uppsala univ (4 ex), Lunds univ, Luleå högskola, LTH, Studsviks Energiteknik AB (3 ex), ASEA, SKI (2 ex), SV (5 ex), OKG (3 ex), Sydkraft (3 ex), InD, FOA 1, FOA 3(2 ex), FOA 4
FOA 2: 202 (100 ex), 210 (2 ex), 283, 284

Index

	Page
Summary	1-4
Index	5
Introduction	6-7
1. Wave propagation within a realistic crust	8
1.1. Crustal model	8
1.2. Attenuation calculations	8-10
1.3. Extended sources	11
2. Acceleration and intensity	11-12
3. Useful transformation of the macroseismic data	12-14
4. Analysis of the macroseismic earthquake data	14-15
5. Calculations of the probability to exceed a given ground acceleration level at a given site	16
5.1. The 1904-earthquake observation	16-18
5.2. The remaining earthquakes	18-20
6. Resulting accelerations for an annual probability of 10^{-5} at the four nuclear power plant sites	21
Discussion	22-23
References	24
Tables	25
Figure captions	26-29
Figures	30-48

Introduction

The construction of nuclear power plants in Sweden has drawn the attention to possible seismic risks in this rather aseismic region.

In the last few years several studies of assigning probabilities to ground accelerations caused by earthquakes in this area and valid for bedrock sites have been published. In this report I present in English the basic ideas of the investigations by Slunga 1976. This paper was presented at the Symposium on Seismic Risk and Neotectonics in Luleå 1977.

As no direct measurements of the accelerations in the near field of large Swedish earthquakes are available, all studies made are relying on relations between intensity and acceleration. The most comprehensive study on this matter seems to have been performed by O'Brien, Murphy and Lahoud, 1976, whose study is based on 1500 strong motion measurements from USA, Europe and Japan.

Instead of working with macroseismic quantities like maximum intensity and radius of perception, we prefer physical quantities such as focal depth and source strength (elastic wave radiating strength). For the purpose of finding a transformation from the macroseismic to the physical quantities, we make theoretical calculations of the wave propagation within a realistic crustal model. The results of these computations determine then our transformation.

As the annual probabilities of interest when discussing nuclear power plants are extremely low, the order of 10^{-5}, the determination of corresponding acceleration levels involves large extrapolations of the observations. By our choice of working with quantities like depth and radiating strength, the extrapolations used will be determined by our assumptions about the distributions of these physical quantities. The assumptions which then completely determines our extrapolations is assumption of linear relation between the cumulative number of earthquakes and the logarithm of the radiating strength, assumption of uniform depth distribution and assumption of uniform epicentral distribution. The latter one is due to the lacking knowledge of the source processes involved and the absence of studies on correlation between seismicity and geological features in Sweden.

As a study on acceleration levels based on macroseismic observations necessarily will be very uncertain, the result will be a range of accelerations assigned to the 10^{-5} annual probability.

No conclusion about acceleration levels will be made in this study as the aim is to present ideas and procedures for determining acceleration levels in low seismicity areas. The determination of acceleration levels to be used for design purposes should not be made without including the wave frequency as an explicit parameter. For doing this more knowledge will be needed than is available today.

1. Wave propagation within a realistic crust

In this chapter we will discuss body wave propagation from uniform point sources in a realistic crustal model. The computational method to be used is given by Bullen 1953. As the S-waves in general are stronger than the P-waves from earthquakes they probably determines the macroseismic observations. The simplest case to handle is the SH-wave. Our computations are thus made for SH-waves. We will restrict the computations to the distance range up to 150 km. For longer distances different surface waves are probably of importance but they are not included in our calculations.

1.1. Crustal model

The attenuation can be divided into geometrical spreading and anelastic attenuation. For the anelastic attenuation we use a Q-factor damping where the value of Q is 800 for depths larger than 5 km.

The geometrical spreading is determined by the velocity distribution within the crust. For simplicity we assume lateral homogenity having the velocity depending only on depth.

The S-velocity as a function of depth has been very little investigated in Scandinavia. We then make the assumption that it has the depth dependence given in figure 1, where we have three zones of stronger velocity increase, the top of the crust, the Conrad- and Moho-discontinuities. Most P-velocity studies can be interpreted in that way. This model of figure 1 is in the following assumed to be representative of the real crust.

1.2. Attenuation calculations

Several models proposed for depth determinations from macroseismic observations implicitly assume a homogenous half space or a constant velocity increase in the crust. In figures 2 and 3 the geometrical spreading is compared for the homogenous half space and the realistic crust of figure 1. We notice that the geometrical spreading for shallow focal depths (h = 8 km) is much stronger for our realistic crustal model.

In figures 4 and 5 attenuation curves are given including both the geometrical spreading and the anelastic attenuation. In figure 4 we have a frequency of 2 Hz and in figure 5 we have 5 Hz. The peak at hypocentral distances of 100 km is due to the Moho-discontinuity.

For the statistical analysis of small Swedish earthquakes we want a simple description of the curves of figure 5. We adopt the following:

$$\log a(R) = C1(h) - C2(h) \log R \qquad 1.1$$

where a(R) is the amplitude (acceleration) at the hypocentral distance R and C1 and C2 are only dependent on the focal depth h. In figure 6 we show the resulting slopes C2 when trying to fit straight lines to the curves of figure 5. The uncertainty of the slopes of these lines is indicated in figure 6. A reasonable analytic approximation of the C2-values is also given in figure 6. When estimating C1(h) we notice that the starting points of the curves of figure 5, that means the acceleration at the epicenters, are given by

$$\log a(h) = C3 - 1.08 \log h \qquad 1.2$$

where the constant C3 is a measure of the source strength, the magnitude. The two formulas 1.1 and 1.2 give together with the approximation of C2(h) of figure 6 the resulting formula

$$\log a(R) = C3 + (0.67 - 0.0004\, h^2) \log h - (1.75 - .0004\, h^2) \log R \qquad 1.3$$

This formula is an approximation calculated for a frequency of 5 Hz, hypocentral distances less than 150 km and assuming a uniformly radiating point source.

By extending our wave propagation calculations out to teleseismic distances we get the result that for sources within the crust, the amplitudes at teleseismic distances are very little dependent on focal depth. This means that the body wave magnitude will be linearly related to our source strength C3. C3 or any linear function of it can thus serve as a magnitude measure.

Our theoretical wave propagation results are essential in this study. As the S-velocity distribution is not very well known and is also difficult to determine from explosion seismology, our wave propagation computations are associated with some uncertainty. The most remarkable feature of the resulting curves in figure 5 is the peaks at hypocentral distances of 100 km. To check if there is any indication of this in our macroseismic observations we plotted in figure 18 the cumulative number of earthquakes as a function of hypocentral distance of perception. There is indeed a small indication of an increased number of earthquakes around 100 km. Huseby and Ringdahl 1977 state that in the distance range 20-60 km and for a frequency of 1.5 Hz an attenuation close to -1.6 logR has been observed at NORSAR and this is also in good agreement with our results of figure 4. The curve h = 8 km of that figure gives an attenuation -1.67 logR and the other curves give less attenuation indicating a focal depth of some 10 km for the NORSAR observations. However, new and more reliable data on the S-wave distribution in the crust is necessary if one wants more reliable attenuation curves.

1.3 Extended sources

The only large earthquake in southern Sweden for the last one hundred years is the earthquake in 1904 having an estimated surface wave magnitude of 6 (Bjerking 1976). This earthquake is certainly not a point source. However, as we are interested in maximum accelerations and they for such a large earthquake probably occur well above the corner frequency, we assume that the high frequency radiation of this earthquake can be described by several point sources. We then assume that the radiation from these distributed point sources is incoherent and thus the maximum acceleration at each point is determined by treating these point sources as single sources and look which one gives the highest acceleration and then adopt this value at the point of interest. If we by this method calculate the attenuation curves for extended sources in upper and lower crust, we get the results in figure 7. In this figure we have only included the extension in depth.

2. Acceleration and intensity

The correlation between intensity and acceleration is weak. Lack of relevant acceleration data for Scandinavia forces us, however, to use macroseismic data for estimating the accelerations in the epicentral area of Swedish earthquakes. Of course the uncertainty will then be considerable and we will therefore give our results in term of acceleration ranges.

As the correlation between intensity and acceleration also seems to be region dependent, the idea will be to take the world mean as the best available relation between intensity and acceleration.

The results derived by O'Brien, Murphy and Lahoud 1976 are well fitted for us as it is based on world wide data. They give the following three relations.

$\log a = 0.40I - 0.85$	$4 \leq I \leq 7$, all distances	2.1
$\log a = 0.38I - 0.56$	$5 \leq I \leq 8$, 25 km	2.2
$\log a = 0.41I - 1.04$	$5 \leq I \leq 8$, 160 km	2.3

where a is expressed in cm/s^2.

The last two formulas indicate a dependence on epicentral distance. We want one formula for the distance range up to 150 km. One way of getting this is by interpolating formulas 2.2 and 2.3. We choose linear interpolation and extrapolation as it gives higher values in the range 25 - 160 km than logarithmic interpolation and a weak distance dependence for small distances. This gives us the relation

$$\log a = 0.40I - 0.0025R + C4 \qquad 2.4$$

where R is hypocentral distance and C4 is a constant.

One should note that O'Brien et al 1976 stated that bedrock sites give acceleration values a factor 1.5 higher than given by formulas 2:1-3. This will be considered in the interpretation of the macroseismic data of the 1904 earthquake.

3. Useful transformations of the macroseismic data

In estimating the statistics of the Swedish earthquakes we will rely on the catalogue by Båth 1956. For each earthquake he gives the maximum intensity Io and the radius of perception. None of these, is taken alone, easy to interpret physically. By combining our results from the wave propagation computations as given in formula 1.3 and the relation between acceleration and intensity as given by formula 2.4 we get

$$I(R) = I + .006(R-h) - (4.4-.001\ h^2) \log (R/h) \qquad 3.1$$

where I(R) is the intensity at hypocentral distance R and h denotes focal depth. This intensity attenuation formula is only valid for distances up to 150 km.

If we assume that the intensity at the radius of perception is known, formula 3.1 can be used to estimate the focal depth h from I_o and the radius of perception.

From the formulas 1.3 and 2.4 we can also deduce the relation

$$\log a = 0.40M + f(h,R) \qquad 3.2a$$

where a is the acceleration at hypocentral distance R from a source at depth h and f(h,R) is a function of h and R while M is constant for a given source strength and is given by

$$M = I_o + 2.7 \log h - 0.006\, h \qquad 3.2b$$

M is a measure of the radiating strength of the source and can thus serve as a magnitude measure. As M is independent of the depth as long as the source strength is the same, formula 3.2b also gives the relation between I_o and focal depth h for a given value of the source strength M. In the following we will use M as defined by 3.2b as a macroseismic magnitude measure. It is related to the constant C3 in the formula 1.2 by a linear relation. This means that our macroseismic magnitude measure for small earthquakes is also linearly related to the body wave magnitude as the constant C3 is so.

These relations between body wave magnitude, the constant C3 and the macroseismic magnitude measure as defined by 3.2b are linear only when our assumption of a point source is true. The only earthquake in our observation sample which cannot be regarded as a point source is the 1904 earthquake. We will later on extrapolate the occurence of large earthquakes from the observations of small earthquakes. We will thereby rely on the general observation of linear relations between the number of earthquakes and instrumental magnitude. Any deviation from the linear relations between the size quantities may affect our extrapolations. In this report we will not try to make a complete investigation on the scaling of body wave magnitude and the macroseismic magnitude. It demands a much more physical approach and the knowledge so far available is not enough for such a description of Swedish earthquakes.

To further check our magnitude definition we compare it to other published relations between magnitude, maximum intensity and focal depth. We thereby note that our formula 3.2b can be approximated

$$M = I_o + C5 \log h$$

where C5 is in the range 2.4 - 2.7.

Karnik 1969 got empirically for northern Europe

$$M = I_o + 2.1 \log h$$

and for other European regions 1.8-2.4 instead of 2.1. He also stated that the magnitude used by him was linearly related to the body wave magnitude. The depths used by Karnik 1969 were determined from macroseismic observations by methods which do not include abrupt changes in the velocity-depth relation.

From these relations we just conclude that our magnitude measure seems to be in reasonable agreement with general experience as it rather well is linearly related to the other formulas.

It is to be noted that our macroseismic magnitude measure is not fully determined but any linear function of it could do as well. The reason for not including the factor 0.4 in the magnitude formula is just to be sure that our magnitude figures will be so large that no one will think of comparing them with magnitude figures determined in any other way.

The formulas 3.1 and 3.2b of this chapter now give a transformation of the macroseismic quantities I_o and radius of perception to the physically more easily interpretable quantities focal depth and radiating strength of the source, (magnitude). In figure 8 we can see the relation between maximum intensity, radius of perception, focal depth and macroseismic magnitude measure when using formulas 3.1 and 3.2b together with the value 2.5 for the intensity at the radius of percpetion.

4. Analysis of the macroseismic earthquake data

Our macroseismic earthquake data will be analysed in terms of focal depth and magnitude measure as given by the relations 3.1 and 3.2b. Using the catalogue by Båth 1956 and restricting ourselves to the circle of figure 9, we get the results of figure 8. Every small circle denotes one earthquake. In figure 10 we compare the depth distribution achieved by our wave propagation results and by a common technique (Huseby and Ringdahl 1977) as given in the figure. From the results obtained can

be seen that our depths are almost all in the range 8-25 km. However, one should note that if the people distribution is not very dense, the probability to identify very shallow depths is small. One can therefore from the results of our macroseismic data not exclude the possiblity of very shallow earthquakes being equally common as deeper ones. From figure 10 a reasonable depth distribution model will then be uniform distribution in the range 0-25 km.

In figure 11 we have plotted the magnitude distribution of the same earthquake sample. The large earthquake in 1904 has not been included but is for discussion marked in the figure with its smallest reasonable macroseismic magnitude measure. The straight line of figure 11 is just fitted by eye and indicates a reasonable slope to use when extrapolating the distribution to larger magnitude measures.

It is obvious from figure 11 that the 1904-earthquake observation does not fit the remaining observations of the 60 years covered by the earthquake catalogue. The latest previous earthquake that might be of similar magnitude was the one in 1759. If we take the mean year to 1759 and 1904, 1831, as a starting point for the time interval to use when estimating the annual number of 1904-magnitude earthquakes we get 1/145 per year instead of 1/60 as indicated in figure 11. However, the straight line of figure 11 gives still a much lower annual number.

When determining the depth of the 1904-earthquake we use the discussion of extended sources in connection to the wave propagation computations. In figure 12 we have marked the intensity decay for the epicentral range 20-70 km for an extended source in either lower or upper crust. The observed intensity decay in this range for the 1904 earthquake seems to be one unit (Austegard 1975) and thus indicates a focal zone in lower crust as the upper crust source gives an intensity decay of two units. This indicates a possible difference between the 1904-earthquake having a depth exceeding 25 km and the smaller ones as most of the latter have focal depths less than 25 km.

5. Calculations of the probability to exceed a given ground acceleration level at a given site

Considering the problems to incorporate the 1904-earthquake in the observations of the smaller earthquakes we decided to split the observations in two groups: one consisting of the 1904-earthquake and one consisting of remaining earthquakes. By doing this we avoid introducing unreasonable conservatism in the calculations without neglecting any observation. As the assumptions necessary for calculating the probabilities associated with the 1904-earthquake are much weaker than the assumptions necessary for evaluating the remaining observations, we start by discussing the 1904-earthquake.

5.1 The 1904-earthquake observation

The idea of this section is to look at earthquakes having the same source strength as the 1904-earthquake. This eliminates the magnitude measure as a variable in our calculations. The variables left are source depth and epicenter coordinates. We also need a formula relating the ground acceleration to hypocentral distance and focal depth.

The most probable focal zone of the 1904-earthquake is the lower crust according to our previous macroseismic discussion. A reasonably conservative depth distribution to use for these earthquakes is then a uniform distribution in the range 0-35 km.

As the source process of the 1904-earthquake is not known and we have no geophysical knowledge today for assigning probabilities to occurrence of a 1904-magnitude earthquake at a certain site, we will rely on the assumption of uniform epicenter distribution. The area of uniform distribution is determined in a conservative way by taking a circle around the site with a radius equal to the distance from the site to the 1904-epicenter. We assume then that we have uniform distribution of 1904-magnitude epicenters within this circle and with a total number of 1/145 eartquakes per year as discussed in the macroseismic interpreta-

tion. Such a procedure of defining the epicenter distribution is conservative if there is no indication of a non-uniform distribution. With this epicenter distribution the seismic risk associated with the 1904-earthquake observation will be a function of the distance to the 1904 epicenter. One should note that use of such conservative procedure for each site cannot be used if we want to look at the total risk for two or more sites. For instance when looking at the site most close to the 1904 epicentre we assume all 1904-size earthquakes to be within a circle not containing all the other sites. For sites not contained within the circle the risk will then be zero. The use of different assumptions for different sites is evidently inconsistent. Actually, if the 1904 earthquake equally well had occured anywhere within, let us say, 500 km of the 1904 epicentre, then all sites within this area have to endure the same seismic risk.

The remaining problem is to determine the acceleration attenuation curve for 1904-earthquake. In figure 13 the wave propagation results for an extended source in upper or lower crust and for a frequency of 2 Hz can be seen. High accelerations will of course only appear at small hypocentral distances and we see from figure 13 that both curves at that part are well approximated by a straight line with slope 1.07. To determine the acceleration level for such a line valid for the 1904-earthquake, we note that according to Svedmark 1909 the maximum observed intensity for 1904-eartquake at bedrock sites seems to be 5 on the Modified Mercalli scale. The hypocentral distance for such observations is less than 60 km. Using this and linear interpolation between the formulas 2.2 and 2.3 we get an acceleration of 0.019 g at epicentral distance 50 km. However, O´Brian et al 1976 also states that the acceleration values for a given intensity is larger by a factor 1.5 on bedrock sites. This gives as a basic assumption in our calculations that the bedrock acceleration at hypocentral distance 60 km of the 1904-earthquake is 0.029 g.

This value 0.029 g is determined from world wide data. As pointed out by O´Brien et al regional variations occur. In all our calculations we therefore include a variation $1.5^{\pm 1}$ of this value and thereby indicate the uncertainties involved in interpreting macroseismic data in terms of acceleration.

The slope 1.07 for a frequency of 2 Hz is changed to 1.15 if a frequency of 4 Hz is used and if we want the straight line to describe the two curves at short distances and at the same time go through the lower crust curve at 60 km hypocentral distance. As a value of 1.15 in this case is more conservative than 1.07 we finally accept the following acceleration attenuation curve for 1904-magnitude earthquake

$$\log a(R) = \log a(1) - 1.15 \log R \qquad 5.1$$

where a(R) is the acceleration in units of g at hypocentral distance R km and log a(1) = 0.507.

We have now stated all assumptions needed and the calculations of the probability of exceeding a given acceleration level is straight-forward by first calculating the annual number of earthquakes giving accelerations at the site above the given level.

In figure 14 we show the results of the acceleration, corresponding to an annual probability 10^{-5}, as a function of distance to the 1904 epicenter. The acceleration range given by the solid lines corresponds to our conservative way of estimating the epicentre distribution while the dotted lines show the lower range achieved if 1904-size earthquakes are equally probable to occur anywhere within the area of figure 9.

Due to our conservative procedure for estimating the uniform epicentral distribution at a given site the acceleration levels will be very high for sites close to the 1904 earthquake. As the last preceding earthquake (1759) having a possibly similar magnitude had another epicentre we think that it is not reasonable to follow the solid curves of figure 14 down to distances less than say 200 km. For sites closer than 200 km we thus propose the 200 km values as reasonable (0.10-0.22 g).

5.2 The remaining earthquakes

This group contains all other earthquakes when the 1904-earthquake is excluded.

As given by our macroseismic interpretation of these earthquakes, a uniform depth distribution in the range 0-25 km seems reasonable and will be used.

For the epicenters we will again assume a uniform distribution where the annual number of earthquakes per sq.km. is estimated by a method similar to the one used for the 1904-earthquake.

To estimate the number of earthquakes having magnitude measures larger than M close to the site we calculate for a circle of radius r the annual number of such earthquakes per sq.km. within the circle.

For different values of r we get different annual numbers per sq.km. We then choose to use the highest annual number given by any radius r less than 450 km. This gives our conservative estimate of the annual number per sq.km. of earthquakes larger than magnitude measure M around the site. These conservative estimates can be plotted as is done in figure 15 for the Oskarshamn nuclear site. We see that the radii used in estimating the numbers are quite large 240 - 390 km indicating the lack of close earthquakes. To these conservative estimates we now fit a straight line with slope -1.1 as found in our macroseismic analysis. The line is determined in such a way that none of our estimated numbers is above the line. We then use the annual number per sq.km as given by the line in our probability calculations. In these calculations we do not use any maximal magnitude but just extrapolate our observations along the straight line.

As we in our calculations will integrate over magnitude measure we choose to use an acceleration attenuation similar to the one used for 1904-magnitude earthquake. We just incorporate the magnitude dependence as given by formula 3.2a in the formula 5.1. For conservativity we thereby use the low value 11.1 as the macroseismic magnitude measure of the 1904-earthquake corresponding to $I_o = 7.5$ and $h = 25$ and get

$$\log a(M,R) = 0.4(M-11.1) + 0.507 - 1.15 \log R \qquad 5.2$$

This formula ca be used to check the consistency of the formulas suggested in this study. Close to the great Lake Vänern in central Sweden an earthquake occured April 11, 1973. This earthquake had a maximum intensity 4-5, say 4.5, and the radius of perceptability was 50 km. From figure 8 this means a focal depth of 15 km and a size measure of 7.7. We put this size value in formula 5.2 and get an epicentral bedrock acceleration of 0.006 g. For this earthquake the maximum observed vertical acceleration at Hagfors array station, at a distance of 160 km, was $5 \cdot 10^{-5}$g for a frequency of 4 Hz. The horizontal acceleration is probably a little larger. To estimate the epicentral acceleration from the Hagfors Observatory we use the 14 km depth curve of figure 5 and get the epicentral bedrock acceleration to be 0.002 g. This is in good agreement with the 0.006 g value above and if we had accepted a higher and actually more likely size value of the 1904 shock the values would be even closer. The epicentral area is covered by sedimentary layers which may amplify the surface acceleration up to 10 times compared to a bedrock surface acceleration (resonance) for small acceleration levels. For an amplification of 5 we get the sedimentary acceleration 0.01 - 0.03 g, which is in agreement with the value 0.01 g given by formula 2.1 for intensity 4.5 (a slight extrapolation). We thus conclude that the formulas proposed here are consistent and in agreement with instrumental observations of small earthquakes.

In the probability calculations we assume that depth, epicenter coordinates and magnitudes are uncorrelated. The calculations are then again straight-forward and this time incorporates an integration over magnitudes.

In figure 16 we see the results for the Oskarhamn site. The wide range given is again due to the factor $1.5^{\pm 1}$ when interpreting the macroseismic observations in terms of accelerations.

6. Resulting accelerations for an annual probability of 10^{-5} at the four nuclear power plant sites

In table 1 the estimated accelerations are given both for each of the earthquake groups and when both are taken together. The large ranges are indicative of the uncertainties involved. Table 1 can be considered as the final result of the probability calculations of this report. To make possible a direct comparison with other studies we give in table 2 the most likely estimate of accelerations for the four sites.

For all sites except Barsebäck the 1904 observation gives higher acceleration than the remaining earthquake observations. This behaviour of the Barsebäck site is due to the fact that during the 60 years time interval on which we base our statistical estimate of the earthquakes a fairly large earthquake occurred within 55 km of this site. As seen in figure 17 this singular observation gives a high seismic activity to the site when our conservative estimating procedure is applied. More reliable estimates at each site may of course be achieved if a larger time interval can be used. We have here only used the data after 1890. This time period can probably be extended further back.

Discussion

The best estimates from this study of acceleration levels at an annual probability of 10^{-5} are .10 - .15 g. One interesting aspect when discussing this acceleration value is to compare it with the acceleration at the epicenter of the 1904-earthquake. From figure 13 can be seen that if we assume the focal zone to be in the depth range 20-35 km and use the 60 km value 0.029 g, we get an epicentral acceleration of 0.09 g and the range 0.06-0.14 g. As most studies of the 1904-eartquake including this one indicate a focal zone in lower crust, this should be a reasonable estimate of the epicentral bedrock accelerations for 1904-earthquake. As one policy for determining the design level is looking at the epicentral acceleration of the largest earthquake of the region, it is interesting to note that this seems to give the same acceleration level as our estimates from the probability model.

We have in this study not included any dispersion in the data. It is a well known fact from seismic observations that fairly large amplitude variations occur for body waves. The reason for not including such a dispersion in the calculations is that we do not know how our acceleration values are related to the dispersion. If we for instance have a logarithmic normal distribution and our curve gives the 50% value the inclusion of dispersion will raise our final acceleration levels. If on the other hand our acceleration curve gives the 75% value (exceeded only in 25% of the observations) then the final acceleration values will be uneffected or even reduced. Our curve is based on the largest observed bedrock intensities and is therefore more likely to be the 75%-value than the 50%-value. The question of what dispersion to use is thus closely connected to the level of our acceleration curve.

In figure 19 the solid lines give the size distribution for the two earthquake distributions we have used, while the dashed line gives the resulting size distribution used when the two earthquake groups are added.

The good agreement between the macroseismic model proposed here and the instrumental observations as discussed in point 5.2 indicate that the results achieved are probably not very far from the truth. The comparison there indicates possibly even lower true accelerations for the group not containing the 1904 shock. The general low acceleration level achieved here is due to our use of bedrock acceleration and not an unspecified ground acceleration. The presence of a low velocity surface layer may amplify the low level bedrock accelerations 5-10 times.

References

Austegaard, 1975	The 1904 earthquake in the Oslofjord area. Appendix C to Dames & Moore report
Bjerking Ingenjörsbyrå and Dames & Moore 1976	Seismic risk analyzis and ground response spectra for the Forsmark area. Uppsala.
Bullen, 1953	An introduction to the theory of seismology, University Press, Cambridge.
Båth, 1956	An earthquake catalogue for Fennoscandia for the years 1891-1950. SGU, Ser C. No 595. Stockholm.
Huseby and Ringdahl, 1977	Seismic risk analysis for the Ringhals, Sweden, nuclear power plant. NTNF/NORSAR, Kjeller, Norway.
Karnik, 1969	Seismicity of the European area. Vol 1, D. Reidel publishing company.
O'Brien, Murphy and Lahoud, 1976	The correlation of peak ground acceleration amplitude with seismic intensity and other physical parameters. Computer Sciences Corporation, Falls Church, Virginia.
Slunga, 1976	Jordskalvsorsakade markskakningar i Forsmark. FOA Rapport C 20099-T1, National Defense Research Institute, Stockholm

Table 1

Acceleration ranges for the annual probability 10^{-5}.

	1904 excluded	only 1904	total
Forsmark	0.04-0.08 g	0.05-0.12 g	0.06-0.13 g
Orskarshamn	0.04-0.08 "	0.06-0.13 "	0.07-0.14 "
Barsebäck	0.08-0.17 "	0.06-0.13 "	0.09-0.20 "
Ringhals	0.05-0.11 "	0.09-0.21 "	0.10-0.21 "

Table 2

Most likely acceleration values for the annual probability 10^{-5}.

Forsmark	0.056 g	0.079 g	0.09 g
Orskarshamn	0.054 "	0.087 "	0.10 "
Barsebäck	0.115 "	0.087 "	0.13 "
Ringhals	0.075 "	0.140 "	0.15 "

Fig. 1 The crustal model used in the wave propagation computations. Q is the anelastic quality factor.

Fig. 2 Theoretical geometrical spreading of the direct wave for a uniformly radiating point source at different depths in a homogenous half space.

Fig. 3 Theoretical geometrical spreading of the direct wave for a uniformly radiating point source at different depths in the realistic crust of figure 1.

Fig. 4 The theoretical distance dependence of the maximal body wave amplitude of a uniformly radiating point source at different depths in a realistic crust. For the anelastic damping a frequency of 2 Hz was used. Note that hypocentral and not epicentral distance is used and that the curves start at the point where the hypocentral distance equals the depth, that means at the epicenter.

Fig. 5 As fig 4 but for a frequency of 5 Hz.

Fig. 6 The approximate values of C2(h) of formula 1.1 are given by the vertical bars for the focal depths of figure 5. The dashed line gives a reasonable analytic approximation for the depth range 0-40 km.

Fig. 7 The theoretical distance dependence of the maximal amplitudes radiated by an extended source consisting of uniformly radiating point sources at different depths. The radiation of the point sources are assumed to be incoherent. The source is only extended in depth. A frequency of 2Hz was used.

Fig. 8 This diagram gives the relations between the two macroseismic quantities, maximal intensity and radius of perception, and the two physically more convenient quantities, focal depth and radiating strength. The radiating strength is expressed as macroseismic magnitude measure defined in formula 3.2b. The solid curves indicate constant maximal intensity and the dashed curves indicate radius of perception. The small circle denote each an earthquake given by Båth 1956 within the circle of figure 9.

Fig. 9 Map of southern Scandinavia. Earthquakes reported by Båth 1956 within the circle have been used in our statistical study. The diameter of the circle is 900 km.

Fig. 10 The cumulative focal depth distribution of the earthquakes within the circle of figure 9. The solid line is achieved by the transformation proposed in this study. The dashed line is achieved by use of the formula given in the figure. The difference is not very significant.

Fig. 11 The small circles give the distribution of the size measure M among the earthquakes within the area of fig. 9 and in the catalogue by Båth 1956. The distribution is described by the number of earthquakes having a size measure exceeding M. The time period is 60 years. The 1904 earthquake has been assigned a smallest reasonable size measure and is not included among the smaller earthquakes. The point 1/145 gives the position of the 1904 earthquake if for that large earthquakes the observed time period is extended. For a discussion of this see the text. The slope of the solid line is just chosen not to be steeper than the slope at the larger M-values.

Fig. 12 This figure shows the distance dependence of the amplitude of an over depth extended source. The solid curve corresponds to a source in lower crust, 20-35 km depth, and the dashed curve corresponds to a source in upper crust, extended over 8-14 km depth. The two points on each of the curves marked by horizontal lines correspond to the epicentral distances 20 and 70 km. The intensity decay over this range is then computed from the formula given in the figure.

Fig. 13 The solid curve gives the distance dependence of the amplitudes from an extended source in lower crust. The dashed curve is the same for a source in upper crust. The dotted line gives the maximal amplitude for any focal depth having the same source strength. The 1904 earthquake is described by the solid curve. The small circle denotes the point used to determine the absolute level of the 1904 curve.

Fig. 14 Resulting acceleration probabilities based on the distribution of 1904-size earthquakes as a function of the distance from the 1904 epicentre. The two solid curves give the acceleration range for the proposed conservative procedure. The dashed lines give the acceleration range when the 1904-size earthquakes are assumed to be equally distributed within a radius of 500 km. The horizontal solid lines give the reasonable acceleration range at small distances when the conservative procedure is adopted.

Fig. 15 The circles give the estimated annual number of earthquakes at the site Oskarshamn having a strength measure exceeding the value at the horizontal axes. The solid line has a fixed slope -1.1 and is adjusted to the observations in such a way that no estimate is above the line.

Fig. 16 The relation between bedrock acceleration to be exceeded and the annual probability. The solid curves give the resulting acceleration range for the Oskarshamn site when the 1904 earthquake is not included. The dashed curve is the most likely value. A bedrock acceleration of 0.05 g is thus exceeded with the annual probability 10^{-5}.

Fig. 17 The same as figure 15 but for the Barsebäck site showing how the single observation of a fairly large earthquake close to a site may raise the conservatively estimated number of earthquakes. In such a case one should try to increase the time period which is possible for larger events.

Fig. 18 The number of earthquakes in the catalogue by Båth 1956 as a function of radius of perception. N_c is the number of earthquakes having a radius exceeding the value given by the horizontal axis.

Fig. 19 The dots give the cumulative size distribution of the earthquakes within the circle of figure 9. The number of earthquakes within the time period studied 60 years, is given. The 1904 earthquake is seperately handled. The frequency of 1904-size shocks is estimated to 1/145 per year from the year of a preceding 1904-size earthquake. The solid sloping straight line shows the estimated distribution of earthquakes when 1904 observations is excluded. The solid lines meeting at the 1904 observation give the estimated distribution of 1904-size earthquakes. The dashed curve is the estimated distribution of the union of the two preceding distributions.

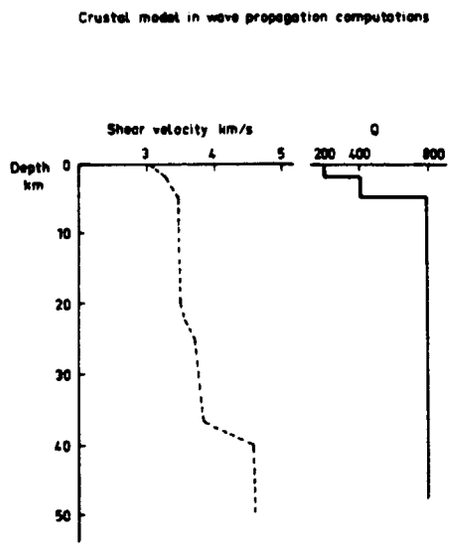

Fig. 1. The crustal model used in the wave propagation computations. Q is the anelastic quality factor.

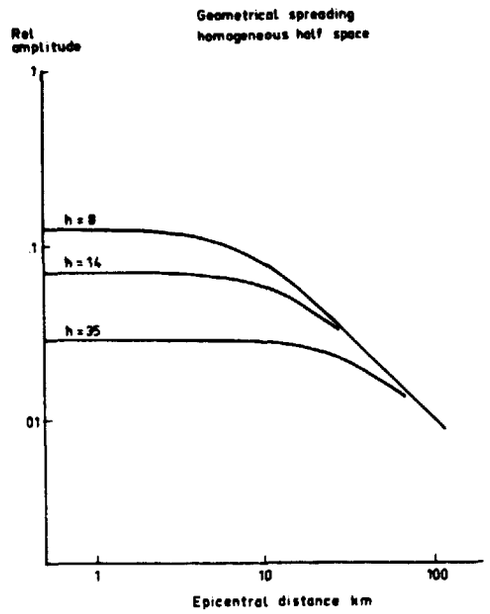

Fig. 2. Theoretical geometrical spreading of the direct wave for a uniformly radiating point source at different depths in a homogenous half space.

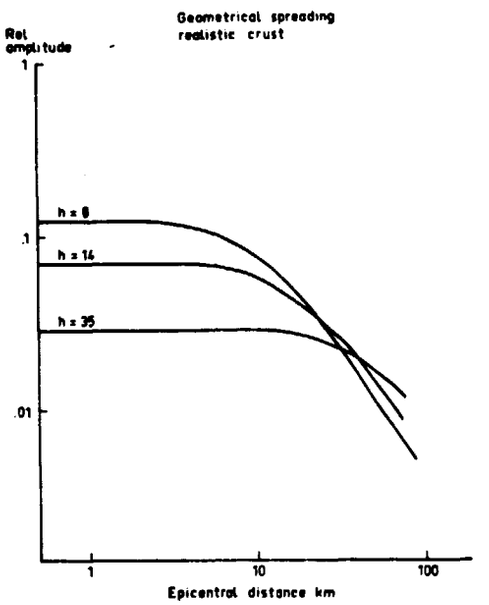

Fig. 3. Theoretical geometrical spreading of the direct wave for a uniformly radiating point source at depths in the realistic crust of figure 1.

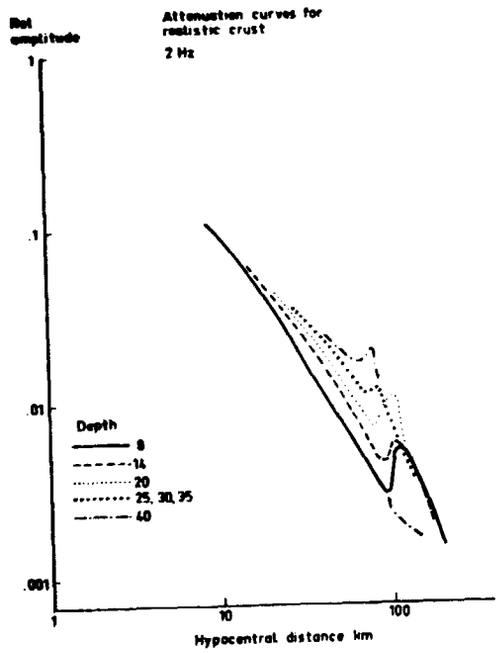

Fig. 4 The theoretical distance dependence of the maximal body wave amplitude of a uniformly radiating point source at different depths in a realistic crust. For the anelastic damping a frequency of 2 Hz was used. Note that hypocentral and not epicentral distance is used and that the curves start at the point where the hypocentral distance equals the depth, that means at the epicenter.

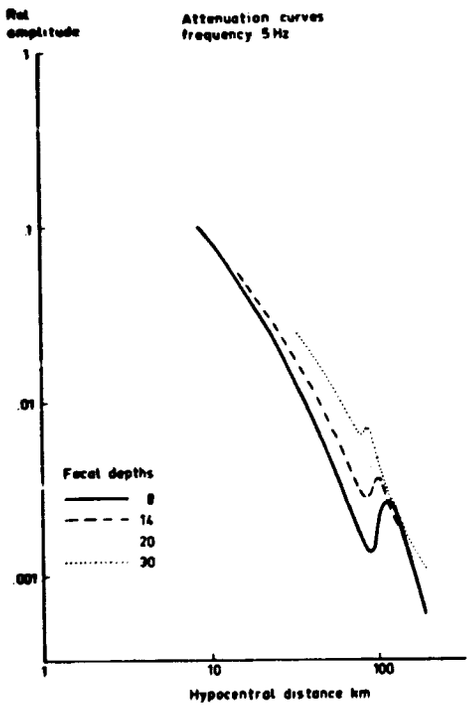

Fig. 5. As fig. 4 but for a frequency of 5 Hz.

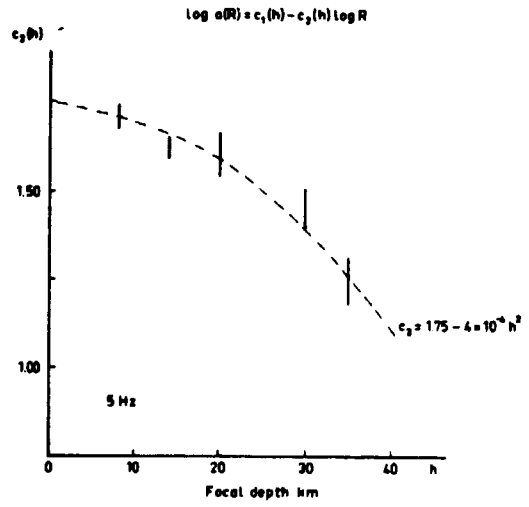

Fig. 6. The approximate values of C2(h) of formula 1.1 are given by the vertical bars for the focal depths of figure 5. The dashed line gives a reasonable analytic approximation for the depth range 0-40 km.

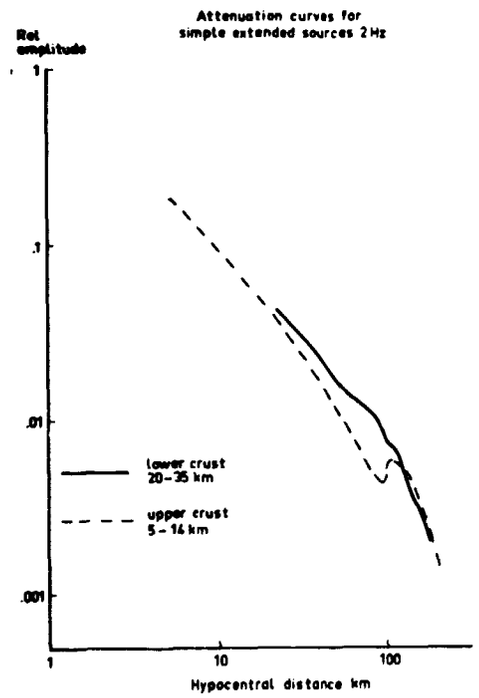

Fig. 7. The theoretical distance dependence of the maximal amplitudes radiated by an extended source consisting of uniformly radiating point sources at different depths. The radiation of the point sources are assumed to be incoherent. The source is only extended in depth. A frequency of 2 Hz was used.

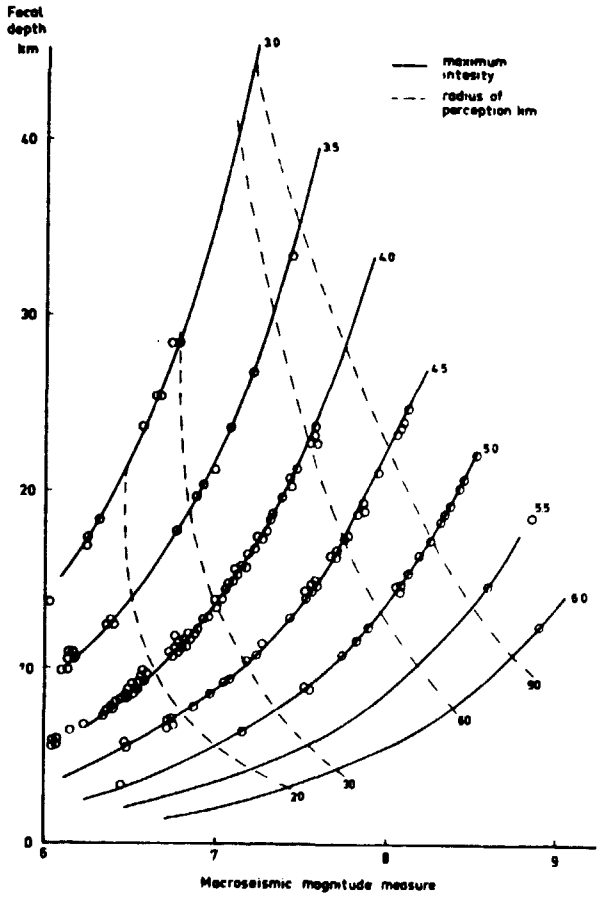

Fig. 8. This diagram gives the relations between the two macroseismic quantities, maximal intensity and radius of perception, and the two physically more convenient quantities, focal depth and radiating strength. The radiating strength is expressed as macroseismic magnitude measure defined in formula 3.2b. The solid curves indicate constant maximal intensity and the dashed curves indicate radius of perception. The small circle denote each an earthquake given by Båth 1956 within the circle of figure 9.

Fig. 9. Map of southern Scandinavia. Earthquakes reported by Båth 1956 within the cricle have been used in our statistical study. The diameter of the circle is 900 km.

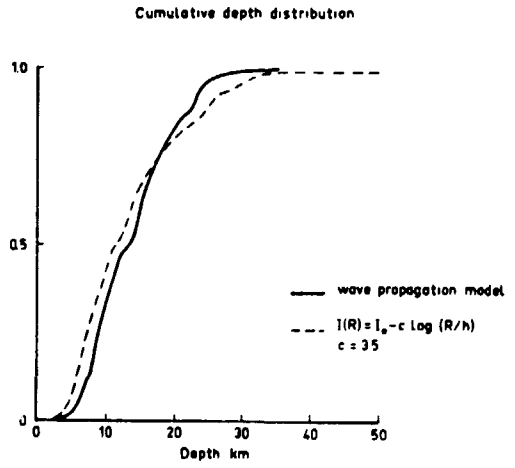

Fig. 10. The cumulative focal depth distribution of the earthquakes within the circle of figure 9. The solid line is achieved by the transformation proposed in this study. The dashed line is achieved by use of the formula given in the figure. The difference is not very significant.

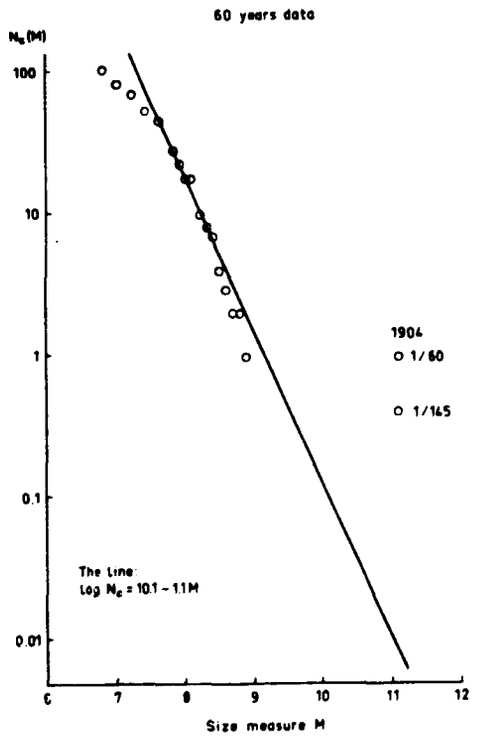

Fig. 11. The small circles give the distribution of the size measure M among the earthquakes within the area of fig. 9 and in the catalogue by Båth 1956. The distribution is described by the number of earthquakes having a size measure exceeding M. The time period is 60 years. The 1904 earthquake has been assigned a smallest reasonable size measure and is not included among the smaller earthquakes. The point 1/145 gives the position of the 1904 earthquake if for that large earthquakes the observed time period is extended. For a discussion of this see the text. The slope of the solid line is just chosen not to be steeper than the slope at the larger M-values.

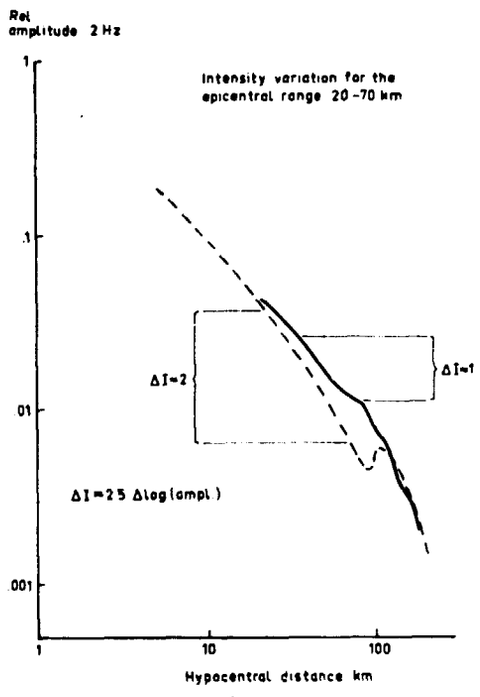

Fig. 12. This figure shows the distance dependence of the amplitude of an over depth extended source. The solid curve corresponds to a source in lower crust, 20-35 km depth, ant the dashed curve corresponds to a source in upper crust, extended over 8-14 km depth. The two points on each of the curves marked by horizontal lines correspond to the epicentral destances 20 and 70 km. The intensity decay over this range is then computed from the formula given in the figure.

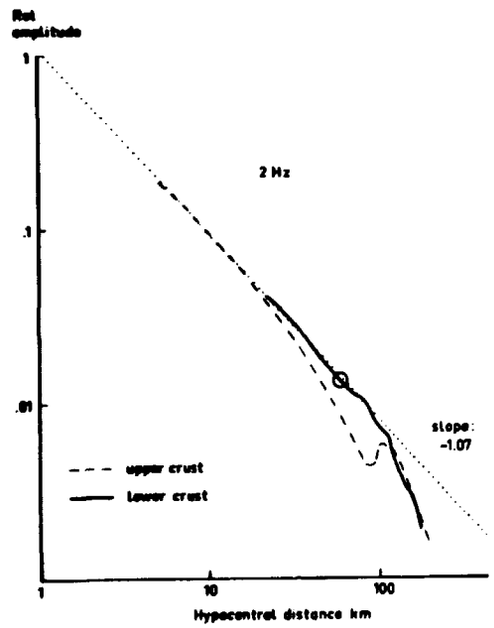

Fig. 13. The solid curve gives the distance dependence of the amplitudes from an extended source in lower crust. The dashed curve is the same for a source in upper crust. The dotted line gives the maximal amplitude for any focal depth having the same source strength. The 1904 earthquake is described by the solid curve. The small circle denotes the point used to determine the absolute level of the 1904 curve.

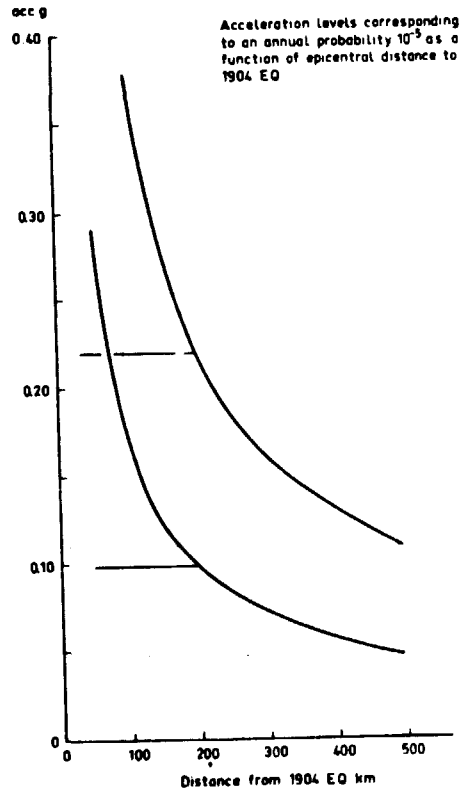

Fig. 14. Resulting acceleration probabilities based on the distribution of 1904-size earthquakes as a function of the distance from the 1904 epicentre. The two solid curves give the acceleration range for the proposed conservative procedure. The dashed lines give the acceleration range when the 1904-size earthquakes are assumed to be equally distributed within a radius of 500 km. The horizontal solid lines give the reasonable acceleration range at small distances when the conservative procedure is adopted.

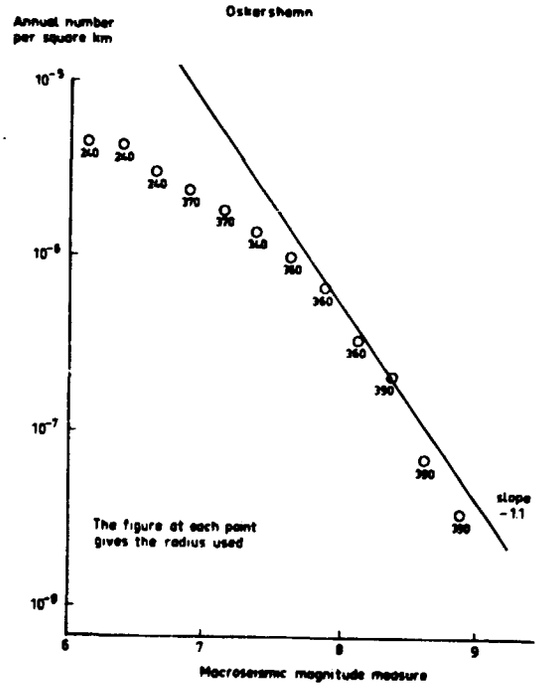

Fig. 15. The circles give the estimated annual number of earthquakes at the site Oskarshamn having a strength measure exceeding the value at the horizontal axes. The solid line has a fixed slope -1.1 and is adjusted to the observations in such a way that no estimate is above the line.

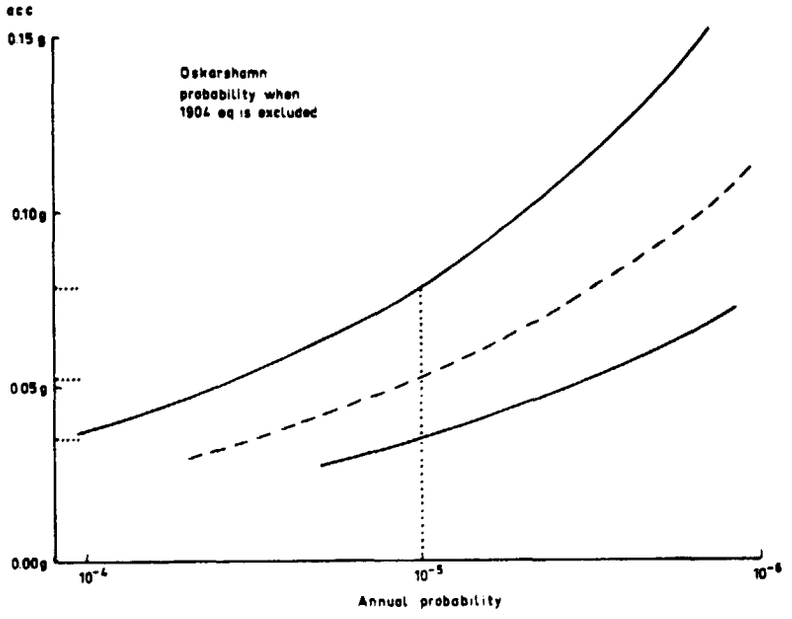

Fig. 16. The relation between bedrock acceleration to be exceeded and the annual probability. The solid curves give the resulting acceleration range for the Oskarshamn site when the 1904 earthquake is not included. The dashed curve is the most likely value. A bedrock acceleration of 0.05 g is thus exceeded with the annual probability 10^{-5}.

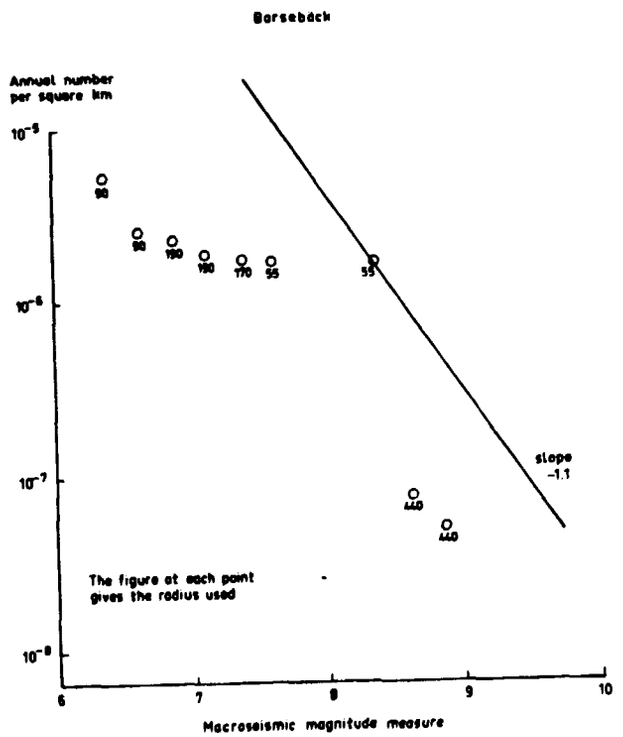

Fig 17. The same as figure 15 but for the Barsebäck site showing how the single observation of a fairly large earthquake close to a site may raise the conservatively estimated number of eartquakes. In such a case one should try to increase the time period which is possible for larger events.

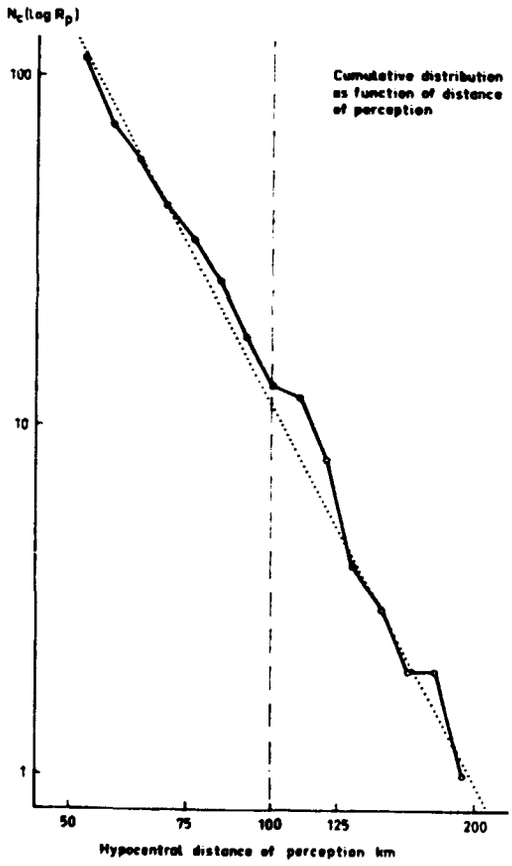

Fig. 18. The number of earthquakes in the catalogue by Båth 1956 as a function of radius of perception. N_c is the number of earthquakes having a radius exceeding the value given by the horizontal axis.

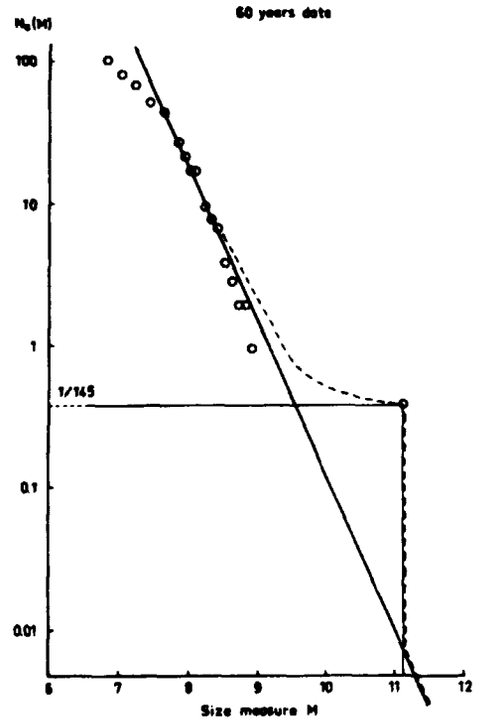

Fig. 19. The dots give the cumulative size distribution of the earthquakes within the circle of figure 9. The number of earthquakes within the time period studied 60 years, is given. The 1904 earthquake is seperately handled. The frequency of 1904-size shocks is estimated to 1/145 per year from the year of a preceding 1904-size earthquake. The solid sloping straight line shows the estimated distribution of earthquakes when 1904 observations is excluded. The solid lines meeting at the 1904 observation give the estimated distribution of 1904-size earthquake. The dashed curve is the estimated distribution of the union of the two preceding distributions.